Latin American Journal of Pharmacy
(formerly *Acta Farmacéutica Bonaerense)*
Lat. Am. J. Pharm. **29** (1): 5-12 (2010)

Original Article

Received: January 16, 2009
Accepted: November 19, 2009

Improving the Phototoxicity of the Zinc Phthalocyanine by Encapsulation in Nanoparticles: Preparation, Characterization and Phototherapy Studies

Mariana V. SOARES, Cíntia M. LANZARINI, Daniely S. OLIVEIRA, Paulo R.S. RAMOS-JÚNIOR, Elizabete P. SANTOS & Eduardo RICCI-JÚNIOR*

Laboratório de Desenvolvimento Galênico (LADEG), Departamento de Medicamentos, Faculdade de Farmácia, Centro de Ciências da Saúde, Universidade Federal do Rio de Janeiro (UFRJ), Av. Brigadeiro Trompowski s/nº, 21941-970, Cidade Universitária, Rio de Janeiro, RJ, Brazil.

SUMMARY. Nanoparticles are widely utilized to overcome drugs insolubility problems and sustain release improving the bioavailability. Zinc phthalocyanine, a hydrophobic photosensitizer with solubility problems, was loaded in PLA nanoparticles. Photosensitizer loaded in polymeric nanoparticles was produced with the following characteristics: size in the 200-300 nm range, negative zeta potential (-15 to -19 mV), low polydispersity index (< 0.1), satisfactory encapsulation efficiency (70-80%), low residual PVA, smooth surface and spherical shape. The photosensitizer release from nanoparticles was sustained and the kinetic followed Higuchi's model. ZnPc loaded in polymeric nanoparticles exhibited higher phototoxicity than free photosensitizer. Phototoxicity of the ZnPc loaded in Resomer® R203 nanoparticles was improved for increasing photosensitizer concentration (1 to 4 μg/ml), light dose (10 to 30 J/cm²) or incubation time (2 to 4 h). The phototoxicity of the zinc phthalocyanine was improved by encapsulation in nanoparticles and this nanocarrier is a promising delivery system for photodynamic therapy use.

INTRODUCTION

Photodynamic Therapy (PDT) is being actively exploited in many clinical applications such as cancer treatment, age related macular degeneration and infections [1]. PDT is based on the administration of drugs known as photosensitizers that are preferentially taken up and/or retained by neoplasic tissues [2]. The photosensitizer alone is harmless and ideally has no effect on either healthy or abnormal tissues. Illumination with visible light at the appropriate wavelength and dose induces photochemical reactions that result in the tissue destruction by apoptosis [3] or necrosis.

Zinc phthalocyanine (ZnPc), a second generation photosensitizer, was used in our experiments due its highly strong phototoxicity [4]. ZnPc is lipophilic and insoluble in water. The hydrophobic characteristic hinders its systemic administration and restricts its clinical studies/application. Nanoencapsulation is a viable alternative in solving the hydro-insolubility problem of some drugs and improving phototoxicity. Several studies have proved that the nanoparticles are promising delivery systems for the photosensitizer. Hexadecafluoro phthalocyanine loaded in polyethylene-glycol-coated polylactic acid (PEG-PLA) nanoparticles induced a better photodynamic effect than the photosensitizer in emulsion on mice EMT-6 tumour cell [5]. Meso-tetra (phydroxyphenyl) porphyrin (pTHPP)-loaded in PLA nanoparticles induced a better phototoxicity than a free photosensitizer on mouse mammary tumour cells 6. Hypericin, a natural photosensitizer, loaded in PLA nanoparticles showed a better phototoxic effect than a free photosensitizer on rat NuTu-19 epithelial ovarian cancer cells [7]. Zinc phthalocyanine loaded in poly-(lactide-co-glycolide) (PLGA) nanoparticles exhibited high phototoxicity on P388-D1 cancer cells (macrophages) after *in vitro* PDT [8].

Biocompatible polymers can be used to pro-

KEY WORDS: Cancer, Nanoparticles, Photodynamic therapy, Photosensitizer.

* Author to whom correspondence should be addressed. *E-mail:* ricci@pharma.ufrj.br

duce nanoparticles. Much attention has been focused on the biodegradable polymers such as polylactic acid (PLA). These synthetic polymers have emerged as the most widely used and studied biodegradable polymers for pharmaceutical use due to their biocompatibility and biodegradability [9]. PLA nanoparticles has been utilized as delivery systems to ferrocenyl tamoxifen [10], paclitaxel [11], indomethacin and magnetic nanoparticles [12] and hypericin [7].

The aim of this work was improve the phototoxic effect of the zinc phthalocyanine by encapsulation in PLA nanoparticles. Photosensitizer was loaded in nanoparticles using PLA with different characteristics (Resomer® R203 and R207). Nanoparticles were characterized for size, charge, morphology, and encapsulation efficiency. *In vitro* release studies were carried out on the nanoparticles to evaluate the photosensitizer availability and kinetic. The phototoxicity of the ZnPc-loaded nanoparticles and free photosensitizer were evaluated on the MCF-7 cancer cells (human breast adenocarcinoma). ZnPc concentration, incubation period and light dose were modified to improve the phototoxic effect.

MATERIALS AND METHODS

Materials

Zinc (II) phthalocyanine and (M_W=577.91) and polyvinyl alcohol hydrolyzed (PVA, 87-89%) (M_W=13,000-23,000) were purchased from Sigma-Aldrich (Milwaukee, USA). Polylactic acids (PLA) (Resomer® R203, M_W 28,000; Resomer® R207, M_W 209,000) were purchased from Boheringer Ingheleim (Germany). Sodium dodecylsulphate (SDS), dichloromethane (DCM), 2-methylpyrrolidone, NaH_2PO_4 and Na_2HPO_4 were purchased from Vetec (Brazil).

Preparation of nanoparticles and Process Yield (%)

Nanoparticles containing ZnPc were prepared by the solvent emulsification evaporation method (SEEM) [8]. About 100 mg of polymer and 0.1, 0.25 or 0.5 mg of ZnPc were briefly dissolved in dichloromethane (DCM). This organic solution was emulsified by an aqueous PVA (3% w/w) solution for 10 min using an ultrasonicator (UP100H, 100 W, 30 kHz, Hielscher, Germany). The solvent (DCM) was evaporated under reduced pressure (Rotavapor, Heidolph, Germany) at room temperature (28 °C). Nanoparticles were purified thrice by a 30 min centrifugation at 20,000 × g (centrifuge J-25, Beckman, USA) for 20 min followed by resuspension in water. The suspension was transferred into a glass vial and frozen in a liquid nitrogen bath. Freeze-drying was carried out in a lyophilizer, yielding powdered nanoparticles. The samples were stored at room temperature (28 °C) before analysis. The process yield was calculated by Equation [**1**]:

$$Y(\%) = (M_{NP}/M_T) \times 100 \qquad [\mathbf{1}]$$

where: Y(%)-process yield, M_{NP}-mass of nanoparticles recovered after freeze-drying, and M_T-mass of polymer plus mass of ZnPc in formulation. The encapsulation method was accomplished in triplicate (n = 3).

Characterization

Nanoparticles were characterized in terms of size, polydispersity index (PI) and charge (zeta potential). The size and PI were determined by photon correlation spectroscopy using a Zetasizer® 5000 (Malvern instruments, UK). The zeta potential was measured in a 10^{-3} M NaCl using the electrophoretic mode with the Zetasizer® 5000. Morphology was determined by Scanning Electron Microscopy (SEM) (Stereoscan 440, Leica, Japan). Nanoparticles were fixed on glass slides and coated with gold prior to examination by SEM.

The encapsulation efficiency was determined by a fluorometric assay. ZnPc was dissolved in pyrrolidone at 100 µg/ml and diluted with isotonic phosphate saline buffer (PBS) at pH 7.4, containing 2% sodium dodecylsulphate (SDS). The analytical curve was prepared in triplicate (n = 3) covering the range of 20-200 ng/ml. The standard solutions were excited at 608 nm and the fluorescence emission spectra recorded between 650 and 800 nm using a fluorimeter (FP 6500, Jasco, Japan). The intensity of fluorescence emission was correlated with the ZnPc concentration (ng/ml). Ten mg of freeze-dried nanoparticles were dissolved in 10 ml of 2-methylpyrrolidone, and 0.5 ml samples were diluted with 2% SDS saline buffer (PBS), and magnetically stirred for an hour at 28 °C. PLA is insoluble in aqueous media and the suspension obtained was centrifuged at 20,000 × g for 20 min (centrifuge J-25, Beckman, USA). The supernatant was collected and ZnPc content measured by the intensity of fluorescence emission as described above. The ZnPc concentrations were measured from the standard curve. Encapsulation efficiency was calculated from Equation [**2**]:

$$EE = (M_1/M_t) \times 100 \qquad [\mathbf{2}]$$

where: EE-encapsulation efficiency, M_1-mass of ZnPc in nanoparticles, and Mt-mass of ZnPc used in formulation. The experiments were accomplished in triplicate (n = 3).

PVA residual was determined using a complexation method of polymer with iodine in presence of boric acid [6]. Nanoparticles (5 mg) were dispersed in 5 ml of 2 N NaOH to hydrolysis of the polymer and neutralized with 2 N HCl. The sample (1.6 ml) was added to 6 ml of boric acid (4%) and 1.2 ml of iodine (1.27% iodine and 2.5% potassium iodide in water). The absorbance of the samples was analyzed at 646 nm and residual PVA was measured using a standard curve.

Releasing studies and kinetic

An amount of PLA nanoparticles containing 50 µg ZnPc was dispersed in 60 ml of 2% SDS phosphate saline buffer (PBS), pH 7.4, at 37 oC. The acceptor solution was stirred with a paddle at a constant rate of 100 rpm, using dissolution equipment (SR8 Plus, Hanson Research). At given time intervals, six samples (n = 6) of 3 ml were withdrawn and centrifuged at 20,000 ×g for 20 min (centrifuge J-25, Beckman, USA). The precipitates were re-suspended in 3 ml of fresh medium and placed in the respective dissolution vessels. Photosensitizer release from the PLA nanoparticles was measured by fluorometric assay (described above) and the intensity of fluorescence emission was utilized to calculate the concentrations of ZnPc. Release profile was obtained correlating time versus photosensitizer release percentage.

The photosensitizer release data obtained from the PLA nanoparticles were fitted utilizing the mathematical models of Zero-order, First-order, Higuchi's model and Hixon-Crowell´s model [13]. Equations of the mathematical modeling are showed in Table 1. Data were fitted and the regression linear of the mathematical modeling was evaluated using R^2. The application of the correct mathematical model allows us analyzed about release rate, points of dissolution change, maximal dissolution of the drugs and mechanisms of drug release.

Function	**Equation**
Zero order	$F=k_0t$
First order	$\ln (1-F)=-k_ft$
Higuchi	$F=k_Ht^{1/2}$
Hixon-Crowell model	$1-(1-F)^{1/3}=k_{1/3}t$

Table 1. Applied mathematical models to the data release of the photosensitizer loaded in nanoparticles. F denotes fraction of drug released up to time t. k_0, k_f, k_H, $k_{1/3}$,$k_{1/2}$, $k_{2/3}$ are constants.

Toxicity and phototoxicity studies

MCF-7 cells (human breast adenocarcinoma) were purchased from American Type Culture Collection (ATCC, USA). The cells were maintained in D-MEM, supplemented with 10% FBS, 50 U/ml penicillin G, 50 µg/ml streptomycin, and 1.0 µg/ml amphotericin B at 37 °C in 5 % CO_2 atmosphere. Aliquots of $2x10^4$ cells were placed into 96-well dishes in 100 µl of culture medium and incubated for 24 h at 37 °C in 5% CO_2 atmosphere before dark toxicity and phototoxicity studies. Free ZnPc was dissolved with 2-methylpirrolidone e diluted in culture medium (0, 1, 2 and 4 µg/ml). Nanoparticles were resuspended in culture medium (0, 1 2 and 4 µg/ml ZnPc). The MCF-7 cancer cells were washed and incubated with ZnPc free or loaded in nanoparticles (0, 1, 2 and 4 µg/ml ZnPc), for 2 h at 37 °C. The cells were then washed and irradiated with red light (675+nm) for 120 s and light dose of 20 J/cm². Irradiation was performed by a laser (Photon Lase I, DMC). After light exposure, the cellular culture was incubated for 24 h at 37 °C in a 5% CO_2 atmosphere and the cellular viability was determined by MTT assay. The dark toxicity and light phototoxicity (0-100 J/cm²) was also determined. The cellular viability was determined by 3-(4,5 dimethyl-thiazol-2-yl-2,5 biphenyl) tetrazolium bromide (MTT). This assay is based on the reduction of the soluble MTT to insoluble formazan (purple) produced by the mitochondrial dehydrogenases present only in living, metabolically active cells. Soon, after removal from the cellular medium, a 50 µl of MTT solution (1 mg/ml) was added to each well and incubated for 3 h. Then, the formazan crystals were dissolved by adding 200 µl of DMSO to each well. The absorbance was determined at 595 nm by a microplate reader. For each sample, the average cellular viability was calculated from the data of ten wells (n = 10) and expressed as a percentage, compared to untreated cells (100%).

Comparison of the mean optical density between untreated (100%) and treated cells 24 h after PDT allowed the evaluation of phototoxicity of ZnPc-loaded nanoparticles in relation to the free photosensitizer. The influence of different parameters on the phototoxicity in vitro was investigated by variation: (i) concentration of

ZnPc free and loaded nanoparticles (0-4 µg/ml), (ii) incubation period of the cell with formulations (0.5-4 h) and (iii) light dose (0-30 J/cm^2).

Statistical analysis

Results were expressed as mean ± SD (standard deviation). The t-test was performed to compare the formulations: ZnPc free and loaded in nanoparticles or ZnPc loaded in Resomer® R203 nanoparticles and Resomer® R207 nanoparticles. The significance of the differences of the phototoxicity studies was calculated and values of $p<0.05$ were considered as significant. All analyses were run using the Graphpad Instat statistical program.

RESULTS AND DISCUSSION

To evaluate the effect of the PLA on the nanoparticles characteristics, two polymers were selected: Resomer® R203 and R207. The nanoparticles were prepared with or without a photosensitizer. Resomer® R203 was loaded with 100, 250 or 500 µg of ZnPc and R207 was loaded with 250 and 500 µg of the photosensitizer. Table 2 shows the influence of the PLA and photosensitizer amount on the nanoparticles characteristics. Satisfactory process yields were obtained (> 60%). The method produced nanoparticles of diameter range between 200 and 300 nm with an excellent polydispersity index (PI < 0.1). Resomer® R203 produced particles smaller than R207. Unloaded nanoparticles are smaller than the ZnPc-loaded nanoparticles. The zeta potential was negative (-12 to -19 mV) for all the formulations. High encapsulation efficiency was obtained utilizing 100 µg of the photosensitizer loaded in Resomer® R203 nanoparticles (>80%). Excellent (> 71%) and satisfactory (> 60%) encapsulation efficiency were obtained utilizing 250 and 500 µg of the photosensitizer, respectively (Table 2).

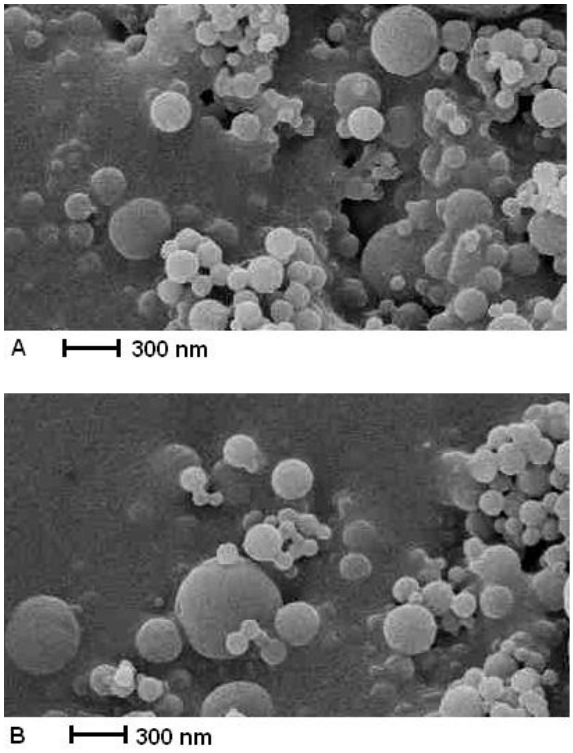

Figure 1. Scanning electronic micrograph from 250 µg of ZnPc-loaded PLA nanoparticles: **A**) Resomer® R203 and **B**) Resomer® R207.

The morphology of the nanoparticles containing 250 µg of ZnPc was examined by SEM and is shown on Figure 1. The PLA nanoparticles have spherical shape, smooth regular surface. The kind of PLA did not influence in the nanoparticles morphology.

The residual PVA of the nanoparticles is shown in Table 2. The purification method removes free polymer (>92%), however, a residual amount remains on the nanoparticles. PVA is a biocompatible polymer but its administration on blood circulation should be minimized. A small amount can help resuspension of the nanoparticles in water after liofilization.

Sample	Polymer	ZnPc (µg)	Size (nm) [a]	(PI) * [b]	Zeta potential (mV) [b]	PVA*** (%, w/w) [b]	E.E. (%)** [a]	Yield (%) [a]
1	RES 203	-	-12.3	5.2	198±7	(0.10)	-	70±1.8
2		100	-13.5	6.3	217±9	(0.07)	83.6±4.2	64±1.5
3		250	-15.4	5.8	205±11	(0.10)	77.5±3.6	63±1.5
4		500	-13.7	7.7	225±6	(0.09)	61.5±2.8	71±3.6
5	RES 207	-	-14.5	6.7	227±8	(0.06)	-	72±1.5
6		250	-18.2	7.3	265±4	(0.08)	71.6±1.6	62±1.7
7		500	-15.3	6.5	268±7	(0.07)	60.6±1.6	64±1.7

Table 2. Characterization of photosensitizer loaded in nanoparticles. [a]: Mean ± S.D. n = 3 determinations; [b]: Mean n = 3 determinations; * PI - Polydispersity Index; ** E.E.: Encapsulation Efficiency; *** Residual PVA in PLA nanoparticles (%, w/w).

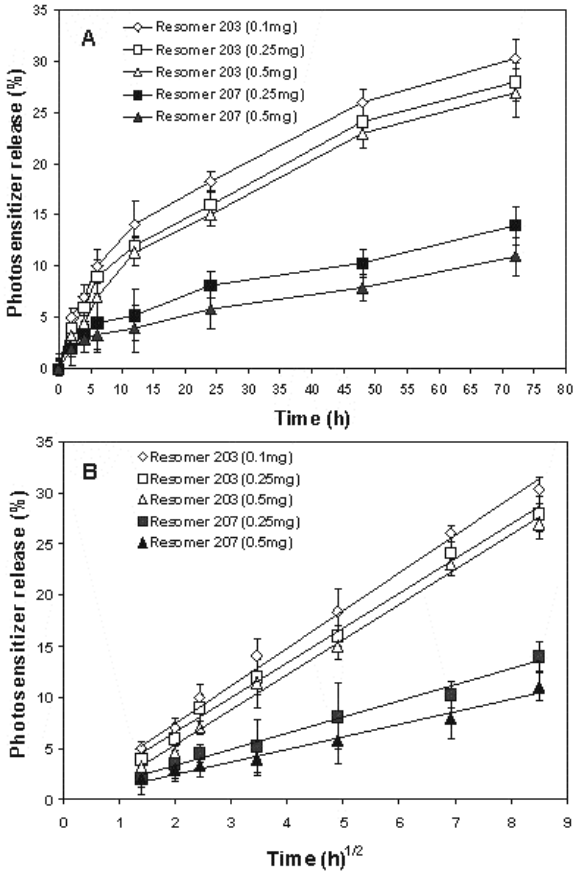

Figure 2. Release profile of ZnPc from PLA (Resomer® R203 and 207) nanoparticles (**A**) and Regression linear of the release data utilizing the Higuchi's model (**B**). Release studies were carried out in 60 ml of isotonic PBS (pH 7,4) containing 2% SDS, at 37 °C, agitation using paddle at a constant rate of 100 rpm. Each point represent the mean ± S.D. of n = 6 determinations.

The *in vitro* release studies are showed in Figure 2A. Photosensitizer exhibited a slow release from nanoparticles in a period of 72 hours. ZnPc release profiles from Resomer® R203 nanoparticles produced with 100, 250 or 500 µg of the photosensitizer are similar (Fig. 2A). The increase of the concentration of the photosensitizer (100 to 500 µg) decreased the encapsulation efficiency and did not modify the photosensitizer release profile (Figure 2A). Similar results were obtained with R207.

Resomer® R207 nanoparticles have slower ZnPc release rate than R203. The results are similar to the results observed in the previous works with others drugs. Docetaxel was loaded in Resomer® R203 or R207 nanoparticles. Nanoparticles were added directly to the dissolution medium in the release studies. Docetaxel release rate from Resomer® R207 nanoparticles was slower than release rate from Resomer® R203 nanoparticles. A sustained release profile was observed and nearly 80% of the drug was release from nanoparticles in 340 h [14].

Several mathematical models have been established to describe the drug release kinetics, and they are used to understand the mechanism of drug release from system [13,15]. Zero-order kinetics can be used to describe the drug release from several types of delivery systems such as matrix tablets for drugs with low solubility [16] and osmotic systems, where drug release would be directly proportional at time. First-order kinetics [17,18] can describe the release profile from the delivery systems containing hydrophilic drugs dispersed in porous matrices, where drugs would be release at the rates proportional to the amounts of drug remaining in the interior of the delivery system [15,19]. Higuchi's model [20] has been based on the Fick's low where the release occurs by the diffusion of drugs within the delivery system. In this case, the cumulative released amount is proportional at square root of time gives the straight line. Hixson-Crowell's cube root model [21] can be applied to the delivery systems whose drug release rate is proportional to the surface area of the system such as the erosion-dependent release systems [22,23]. As shown in Table 3, Higushi's model gave the

Release mathematical models	**Parameters**	**1**	**2**	**3**	**4**	**5**
Zero order	R^2	0.9381	0.9472	0.9464	0.9552	0.9693
First order	R^2	0.9561	0.9621	0.9615	0.9612	0.9728
Higuchi	R^2	0.9936	0.9943	0.9940	0.9849	0.9813
Hixon-Crowell model	R^2	0.9505	0.9574	0.9565	0.9593	0.9717

Table 3. Squared correlation coefficient (R2) obtained after linear regression of the release data utilizing four mathematical models. R^2: squared correlation coefficient; **1**: ZnPc-loaded Resomer® R203 nanoparticles (photosensitizer mass of 100 µg); **2**: ZnPc-loaded Resomer® R203 nanoparticles (photosensitizer mass of 250 µg); **3**: ZnPc-loaded Resomer® R203 nanoparticles (photosensitizer mass of 500 µg); **4**: ZnPc-loaded Resomer® R207 nanoparticles (photosensitizer mass of 250 µg); **5**: ZnPc-loaded Resomer® R203 nanoparticles (photosensitizer mass of 500 µg).

highest value of the squared correlation coefficient (R^2), indicating that this mathematical model would be the most suitable model for describing the release of the photosensitizer from PLA nanoparticles. Figure 2B show the linear regression of the release data obtained utilizing the Higuchi's model. This result suggests that the release of the photosensitizer from PLA nanoparticles is controlled by the diffusion. From these results, the mechanism of the photosensitizer release from PLA nanoparticles can be considered as follows: 1) water penetrates into polymeric matrix of the nanoparticles through porous slowly dissolving the photosensitizer, 2) zinc phthalocyanine is released by diffusion to acceptor solution and 3) photosensitizer is hydrophobic and accumulates into SDS micelles.

Nanoparticles have been chosen as vehicles for delivery of photosensitizers because: they can transport hydrophobic drugs in blood, their large surface area can be modified with functional groups for additional chemical/biochemical properties, they have large volumes of distribution and are generally taken up efficiently by cells and controlled release of the drug is possible [24,25].

No toxicity was observed in controls where cells were incubated with polymeric nanoparticles without photosensitizer. No dark toxicity of ZnPc free or loaded in Resomer® R203 or R207 nanoparticles was detected in the range of 0.5 to 4 µg/ml (figure not shown). Light alone (0-100 J/cm2) was also harmless to the cells (not shown).

The phototoxicity of different concentrations of free ZnPc and loaded in Resomer® R203 and R207 nanoparticles was evaluates in cancer cells culture and compared with free photosensitizer. For all studied formulations, cell viability decreased with increase in the photosensitizer concentrations in the range of 1 to 4 µg/ml. No phototoxicity was observed at 0.5 µg/ml (Fig. 3). From the range 1 to 4 µg/ml, ZnPc-loaded Resomer® R203 nanoparticles exhibited a phototoxicity significantly higher than free photosensitizer ($p < 0.05$) (Fig. 3). ZnPc-loaded Resomer® 207 nanoparticles showed phototoxicity similar to free photosensitizer in the range of 1 to 2 µg/ml and in the concentration of 4 µg/ml exhibited a phototoxicity significantly higher than free photosensitizer ($p < 0.05$). At concentration of 4 µg/ml, ZnPc-loaded Resomer® R203 nanoparticles exhibited a 6 fold higher phototoxicity than free photosensitizer. Resomer® R203 nanoparticles were selected to complementary studies of light dose and incubation time.

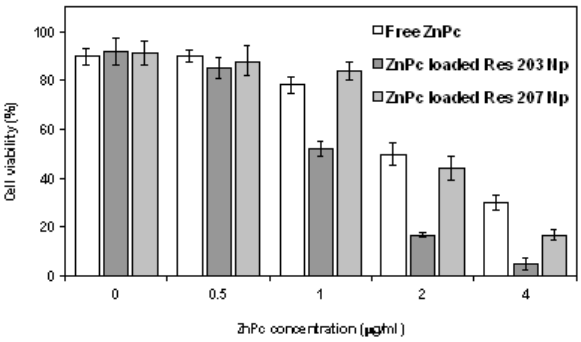

Figure 3. Influence of the photosensitizer concentration on phototoxicity of free ZnPc or loaded nanoparticles. The cells were incubated for 2 h at equivalent photosensitizer doses ranging from 0 to 4 µg/ml and irradiated at a light dose of 20 J/cm². MTT assay was performed 24 h after light exposure. Each data point represents the mean (± S.D.) of n = 10 determinations.

The *in vitro* results showed that photosensitizer encapsulation in nanoparticles improved the phototoxicity. The different phototoxicity of the free ZnPc in solution and loaded in nanoparticles is explained by the difference in the cellular localization and aggregation in the dimmer form. In solution, free lipophilic photosensitizer is generally up-taken by diffusion across the plasmatic membrane (lipophilic) leading to a low intracellular concentration. In aqueous medium, ZnPc can aggregate in dimmers with reduction of phototoxic activity. In contrast, nanoparticles are up-taken by endocytosis by the cells. Endocytosis of the ZnPc-loaded polymeric nanoparticles may lead to higher intracellular concentration of the photosensitizer whereas free ZnPc, due to its hydrophobic nature, tends to diffuse passively into the cell membrane, where it is less active. ZnPc exhibited slow release from nanoparticles preventing the formation of the dimmers.

The phototoxic effect was influenced by the polymer molecular weight. Resomer® R203 nanoparticles was more efficient than R207 (Fig. 4). In this case, Resomer R203 and R207 nanoparticles possess similar characteristics in terms particle size, negative zeta potential, morphology and encapsulation efficiency. However, nanoparticles produced with Resomer® R203 (small molecular weight) have a higher release rate and thus phototoxic effect.

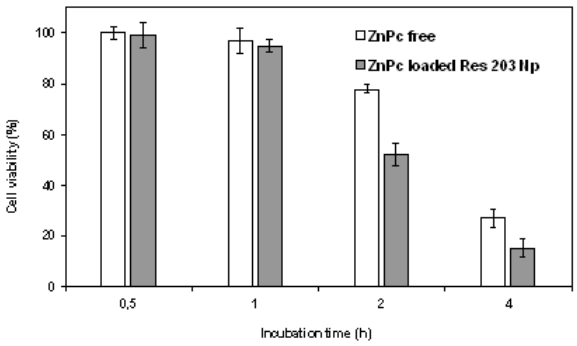

Figure 4. Influence of incubation time on photoactivity of free ZnPc and loaded Resomer® R203. The cells were incubated for increasing incubation times (30 min to 4 h), at an equivalent drug dose of 1 μg/ml, and irradiated at a light dose of 20 J/cm². MTT assay was performed 24 h after light exposure. Each data point represents the mean (±S.D.) of n = 10 determinations.

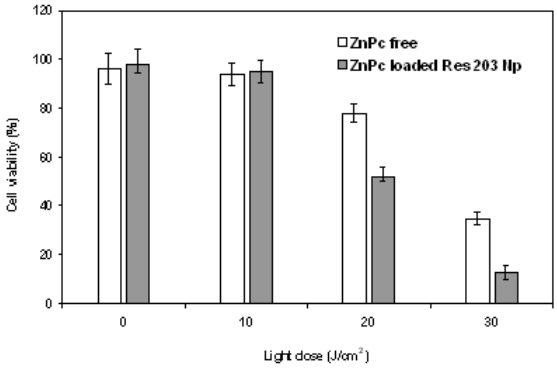

Figure 5. Influence of light dose on phototoxicity of free ZnPc and loaded RES 203. The cells were incubated for increasing incubation times 2 h, at an equivalent drug dose of μg/ml, and irradiated at a light dose from 0 to 30 J/cm². MTT assay was performed 24 h after light exposure. Each data point represents the mean (±S.D.) of n = 10 determinations.

The phototoxicity efficiency of ZnPc loaded in nanoparticles is dependent on the polymer nature. Resomer® R203 (PLA) and PLGA have different characteristics such as hydrophilicity, water accessibility, drug release rate, matrix erosion rate and polymer degradation rate. Ricci & Marchetti [8] loaded ZnPc in PLGA nanoparticles utilizing SEEM and the development system was able to inactivate 60% of the P388-D1 cells in culture medium after phototherapy. The cancer cells were incubated with nanoparticles corresponding at 2.89 μg/ml of ZnPc by 6 h and illuminated with light (675 nm) by 120 s and light dose of 30J/cm². ZnPc loaded in Resomer® R203 nanoparticles produced by SEEM inactivated 83% of the MCF-7 cells. The photoretapy conditions were incubation with nanoparticles corresponding at 2 μg/ml of ZnPc by 2 h and illuminated with light (675 nm) by 120 s and light dose of 20J/cm². The nanostructured system produced with Resomer® R203 was more efficient because utilized small photosensitizer concentration and light dose.

The influence of incubation period and light dose on the phototoxicity was evaluated at a concentration of 1 μg/ml for incubation times ranging from 0.5 to 4 h and light doses from 0 to 30 J/cm². The incubation time reflects the kinetics of cellular uptake of the dye or delivery system, short incubation time may suggest a rapid uptake of the nanostructured systems by cancer cells [6]. At 1 μg/ml, the first phototoxicity was observed after 2 h of incubation for both studied formulations (Fig. 4). A significant difference on the cell viability was observed between 1 and 2 h ($p < 0.05$) and 2 and 4 h ($p < 0.05$). In the incubation time of 2 or 4 h, ZnPc-loaded Resomer® R203 nanoparticles exhibited a phototoxic effect significantly higher than free photosensitizer ($p < 0.05$) (Fig. 4). No phototoxicity was observed to incubation time of 0.5 and 1 h evidencing a low cellular uptake of the ZnPc free or nanostructured system. ZnPc is photoactive after cellular uptake and accumulate in plasmatic membrane, mitochondria, nucleus and lissosome. Phototoxicity was observed after 20 J/cm² exhibiting a phototoxic effect significantly higher than free photosensitizer ($p < 0.05$) (Figure 5). No phototoxic effect was observed below 10 J/cm². The incubation time might be even shortened by increase of the light dose from 20 to 30 J/cm² since the phototoxicity of ZnPc loaded in nanoparticles was improved at 2 h of incubation compared with the free photosensitizer (Fig. 5). A rise in the light dose 1.5 times is enough to increase 4 times cell death. High percentage of cellular death (85%) may be achieved utilizing long incubation time (4 hours incubation, 20 J/cm²) or rise dose light (30 J/cm², 2 hours incubation).

CONCLUSION

The nanoencapsulation method was suitable for the preparation of PLA nanoparticles. Photosensitizer has a slow release from nanostructured systems. Encapsulation of ZnPc in the PLA nanoparticles improved its in vitro phototoxicity. The phototoxicity was influenced by the PLA and photodynamic parameters such as incubation period, light dose and drug concentration.

Low photosensitizer concentration of ZnPc loaded in Resomer R203 nanoparticles was required to obtain an excellent phototoxicity after phototherapy. ZnPc loaded in Resomer® R203 nanoparticles were more phototoxic than free photosensitizer and loaded in Resomer® R207 nanoparticles. Phototoxic effect of the free ZnPc or loaded in Resomer® R203 nanoparticles was improved by the increase of the incubation period and light dose. All the photobiological measurements performed allow us conclude that ZnPc-loaded Resomer® R203 nanoparticles is a promising photosensitizer delivery system for the photodynamic therapy.

Acknowledgements. We would like thank the financial support of FAPERJ (Fundação de Amparo à Pesquisa do Estado do Rio de Janeiro) and CNPq (Conselho Nacional de Desenvolvimento Científico e Tecnológico).

REFERENCES

1. Allison, R.R., H.C. Mota, V.S. Bagnato & C.H. Sibata (2008) *Photodiagn. Photodynam. Ther.* **5**: 19-28.
2. Castano, A.P., T.N. Demidova & M.R. Hamblim (2005) *Photodiagn. Photodynam. Ther.* **2**: 91-106.
3. He X.Y., R.A. Sikes, S. Thomsen, L.W. Chung & S.L. Jacques (1994) *J. Photochem. Photobio. B.* **59**: 468-73.
4. Bonnett, R. (1995) *Chem. Soc. Rev.* **210**: 19-33.
5. Allémann, E., J. Rousseau, N. Brasseur, S.V. Kudrevich, K. Lewis & J.E. van Lier (1996) *Int. J. Cancer.* **66**: 821-4.
6. Konan, Y.N., R. Cerny, J. Favet, M. Berton, R. Gurny & E. Allémann (2003) *Eur. J. Pharm. Biopharm.* **18**: 241-9.
7. Zeisser-Labouèbe, M., N. Lange, R. Gurny & F. Delie (2006) *Int. J. Pharm.* **326**: 174-81.
8. Ricci-Júnior, E. & J.M. Marchetti (2006) *Int. J. Pharm.* **310**: 187-195.
9. Soppimath, K.S., T.M. Aminabhaui, A.R. Kulkarni & W.E. Rudzinski (2001) *J. Control. Release.* **70**: 1-20.
10. Nguyen, A., V., Marsaud, C. Bouclier, S. Top, A. Vessieres, P. Pigeon, R. Gref, P. Legrand, G. Jaouen & J.M. Renoir (2008) *Int. J. Pharm.* **347**: 128-35.
11. Lee, L.Y., C.H. Wang & K.A. Smith (2008) *J. Control. Release* **125**: 96-106.
12. Závisová, V., M. Koneracká, O. Štrbák, N. Tomašovičová, P. Kopčanský, M. Timko & I. Vavra (2007) *J. Magn. Magn. Mater.* **311**: 379-82.
13. Barzegar-Jalali, M., K. Adibkia, H. Valizadeh, M.R.S. Shadbad, A. Nokhodchi, Y. Omidi, G. Mohammadi, S.H. Nezhadi & M. Hasan (2008) *J. Pharm. Pharm. Sci.* **11**: 167-77.
14. Musumeci, T., C.A. Ventura, I. Giannone, B. Ruozi, L. Montenegro, R. Pignatello & G. Puglisi (2006) *Int. J. Pharm.* **325**: 172-9.
15. Tanaka, N., K. Imai, K. Okimoto, S. Ueda, Y. Tokunaga, A. Ohike, R. Ibuki, K. Higaki & T. Kimura (2005) *J. Control. Release.* **108**: 386-95.
16. Varelas, C.G., D.G. Dixon & C. Steiner (1995) *J. Control. Release.* **34**: 185-92.
17. Gibaldi, M. & S. Feldman (1967) *J. Pharm. Sci.* **56**: 1238-42.
18. Wagner, J.G. (1969) *J. Pharm. Sci.* **58**: 1253-7.
19. Mulye, N.V. & S.J. Turco (1995) *Drug Dev. Ind. Pharm.* **21**: 943-53.
20. Higuchi, T. (1963) *J. Pharm. Sci.* **52**: 1145-9.
21. Hixson A.W. & J.H. Crowell (1931) *Ind. Eng. Chem. Res.* **23**: 923-31.
22. Costa, P. & J.M.S. Lobo (2001) *Eur. J. Pharm. Sci.* **13**: 123-3.
23. Yan, G., H. Li, R. Zhang & D. Ding (2000) *Drug Dev. Ind. Pharm.* **26**: 681-6.
24. Bechet, D., P. Couleaud, C. Frochot, M.L. Viriot, F. Guillemin & M. Barberi-Heyob (2008) *Trends Biotechnol.* **26**: 612-21
25. Chatterjee, D.K., L.S. Fong & Y. Zhang (2008) *Adv. Drug Deliver. Rev.* **60**: 1627-37.